

TECHNICAL
LIBRARY

AD

TECHNICAL REPORT ARLCB-TR-80040

NUMERICAL PREDICTION OF RESIDUAL STRESSES
IN AN OVERLOADED BREECH RING

P. C. T. Chen .

October 1980



US ARMY ARMAMENT RESEARCH AND DEVELOPMENT COMMAND
LARGE CALIBER WEAPON SYSTEMS LABORATORY
BENET WEAPONS LABORATORY
WATERVLIET, N. Y. 12189

AMCMS No. 36KA7000204

DA Project No. 156401813GRN

PRON No. 1A0215641A1A

APPROVED FOR PUBLIC RELEASE; DISTRIBUTION UNLIMITED

DISCLAIMER

The findings in this report are not to be construed as an official Department of the Army position unless so designated by other authorized documents.

The use of trade name(s) and/or manufacturer(s) does not constitute an official indorsement or approval.

DISPOSITION

Destroy this report when it is no longer needed. Do not return it to the originator.

REPORT DOCUMENTATION PAGE		READ INSTRUCTIONS BEFORE COMPLETING FORM
1. REPORT NUMBER ARLCB-TR-80040	2. GOVT ACCESSION NO.	3. RECIPIENT'S CATALOG NUMBER
4. TITLE (and Subtitle) NUMERICAL PREDICTION OF RESIDUAL STRESSES IN AN OVERLOADED BREECH RING		5. TYPE OF REPORT & PERIOD COVERED
		6. PERFORMING ORG. REPORT NUMBER
7. AUTHOR(s) P. C. T. Chen		8. CONTRACT OR GRANT NUMBER(s)
9. PERFORMING ORGANIZATION NAME AND ADDRESS Benet Weapons Laboratory Watervliet Arsenal, Watervliet, NY 12189 DRDAR-LCB-TL		10. PROGRAM ELEMENT, PROJECT, TASK AREA & WORK UNIT NUMBERS AMCMS No. 36KA7000204 DA Project No. 156401813GRN PRON No. 1A0215641A1A
11. CONTROLLING OFFICE NAME AND ADDRESS US Army Armament Research & Development Command Large Caliber Weapon Systems Laboratory Dover, NJ 07801		12. REPORT DATE October 1980
		13. NUMBER OF PAGES 19
14. MONITORING AGENCY NAME & ADDRESS (if different from Controlling Office)		15. SECURITY CLASS. (of this report) UNCLASSIFIED
		15a. DECLASSIFICATION/DOWNGRADING SCHEDULE
16. DISTRIBUTION STATEMENT (of this Report) Approved for public release; distribution unlimited.		
17. DISTRIBUTION STATEMENT (of the abstract entered in Block 20, if different from Report)		
18. SUPPLEMENTARY NOTES Presented at 1980 Army Numerical Analysis and Computer Conference, NASA Ames Research Center, Moffett Field, California, 20-21 February 1980. Published in proceedings of the conference.		
19. KEY WORDS (Continue on reverse side if necessary and identify by block number) Breech Ring Residual Stress Numerical Technique Elastic-Plastic		
20. ABSTRACT (Continue on reverse side if necessary and identify by block number) This report describes a numerical technique for predicting the residual stresses in an overloaded breech ring. The numerical approach used is the finite element method based on the incremental stress-strain matrix, for which a computer program is developed. The material behavior is characterized by the von Mises' yield criterion, Prandtl-Reuss flow equations and isotropic hardening rule. A piecewise linear representation for the stress-strain (CONT'D ON REVERSE)		

20. Abstract (Cont'd)

curve is used. The numerical results of the stresses in all elements are obtained for four contact conditions. The location and magnitude of the maximum fillet stress are determined as a function of loading. Residual stresses resulting from elastic unloading are calculated. A satisfactory agreement between numerical and experimental results has been reached.

TABLE OF CONTENTS

	<u>Page</u>
INTRODUCTION	1
METHOD AND PROGRAM	2
MODEL AND LOADING	5
RESULTS AND DISCUSSIONS	8
REFERENCES	11

LIST OF ILLUSTRATIONS

1. A Finite Element Model for Breech Ring.	12
2. Major Principal Stress Along the Boundary Elements for Case 1.	13
3. Major Principal Stress Along the Boundary Elements for Case 2.	14
4. Major Principal Stress Along the Boundary Elements for Case 3.	15
5. Major Principal Stress Along the Boundary Elements for Case 4.	16
6. Determination of the Maximum Tensile Stress for Case 2.	17
7. Stresses in Element 99 as Functions of Contact Force for Case 2.	18

INTRODUCTION

In guns with a sliding breech mechanism, breech ring failures have been observed originating from the lower fillet in the vicinity of the contact region. The observations indicate that high tensile stress produced by stress concentration at the fillet was responsible for the failure. In order to reduce the chance of failure and extend the fatigue life, an exploratory study was initiated on the autofrettage of a breech mechanism. The technique is based on the production of beneficial residual stresses through coldworking to counteract the high operating stresses induced by firing.

A photoplastic model made of aluminum block and polycarbonate ring was designed.¹ The maximum fillet stresses for an elastic load, as well as an elastoplastic load, were determined experimentally. Residual stress resulting from removing maximum test load was calculated. A numerical investigation of the photoplastic model was made by using NASTRAN.² The numerical results are in good agreement with the experimental data in the elastic range of loading, but not in the plastic range. The NASTRAN program stops before the maximum test load is reached, thus residual stress after complete unloading cannot be calculated.

This report describes a numerical technique for predicting the residual stresses in an overloaded breech ring. The numerical approach used is the finite element method based on the incremental stress-strain matrix, for which

¹Cheng, Y. F., "Photoplastic Study of Residual Stress in an Overloaded Breech Ring," Technical Report ARLCB-TR-78018, November 1978.

²Chen, P. C. T. and O'Hara, G. P., "NASTRAN Analysis of a Photoplastic Model for Sliding Breech Mechanism," Proceedings 1979 Army Numerical Analysis and Computer Conference, pp. 237-254.

a computer program is developed. The material behavior is characterized by the von Mises' yield criterion, Prandtl-Reuss flow equations and isotropic hardening rule. A piecewise linear representation for the stress-strain curve is used. The numerical results of the stresses in all elements are obtained for four contact conditions. The location and magnitude of the maximum fillet stress are determined as a function of loading. Residual stresses resulting from elastic unloading are calculated. A satisfactory agreement between numerical and experimental results has been reached.

METHOD AND PROGRAM

The finite element method used here is of the incremental type since solutions to problems involving nonlinear material are best obtained by solving a sequence of linear problems associated with an incremental application of loading. The formulation of the governing matrix equation is developed by using the incremental stress-strain matrix in conjunction with the stationary principle for elastic-plastic solids. Following the procedure outlined in reference 3, we have developed a finite element computer program for solving two-dimensional elastic-plastic problems of rotational symmetry. The element type is either triangular⁴ or quadrilateral⁵, and both were implemented in

³Yamada, Y., Yoshimura, N., and Sakurai, T., "Plastic Stress-Strain Matrix and Its Application for the Solution of Elastic-Plastic Problems by the Finite Element Method," International Journal of Mechanical Science, Vol. 10, pp. 343-354, 1968.

⁴Chen, P. C. T., "Elastic-Plastic Solution of a Two-Dimensional Tube Problem by the Finite Element Method," Transactions of Nineteenth Conference of Army Mathematicians, ARO Report 73-3, pp. 763-784, 1973.

⁵Chen, P. C. T., "Numerical Solution of Gun Tube Problems in the Elastic-Plastic Range," Proceedings 1977 Army Numerical Analysis and Computer Conference, pp. 423-439.

analyzing gun tube problems. For the present problem, the plane stress case was implemented. The field displacement is based on the linear displacement function in a triangular element. Small strain condition is used to derive the kinematical matrix [B]. The material behavior is characterized by the von Mises' yield criterion, Prandtl-Reuss flow equations and isotropic hardening rule. A piecewise linear representation for the effective stress-strain curve is used. As derived in reference 3, the incremental form of the constitutive matrix [D] for an elastic-plastic element ($\sigma > \sigma_0$) can be written as

$$\begin{aligned} \{\Delta\sigma\}^T &= [D] \{\Delta\varepsilon\} \\ \{\Delta\sigma\}^T &= \Delta\sigma_x, \Delta\sigma_y, \Delta T_{xy} \\ \{\Delta\varepsilon\}^T &= \Delta\varepsilon_x, \Delta\varepsilon_y, \Delta\gamma_{xy} \end{aligned}$$

and

$$[D] = \frac{E}{A_3} \begin{bmatrix} \sigma_y'^2 + 2A_1 & & & \text{SYM.} \\ -\sigma_x'\sigma_y' + 2\nu A_1 & , & \sigma_x'^2 + 2A_1 & \\ -\frac{\sigma_x' + \nu\sigma_y'}{1+\nu} T_{xy} & , & -\frac{\sigma_y' + \nu\sigma_x'}{1+\nu} T_{xy} & , & \frac{A_2}{2(1+\nu)} + \frac{2H'(1-\nu)\sigma}{9E} \end{bmatrix} \quad (1)$$

where E, ν are Young's modulus, Poisson's ratio, respectively.

³Yamada, Y., Yoshimura, N., and Sakurai, T., "Plastic Stress-Strain Matrix and Its Application for the Solution of Elastic-Plastic Problems by the Finite Element Method," International Journal of Mechanical Science, Vol. 10, pp. 343-354, 1968.

$$\begin{aligned}
A_1 &= \frac{2H'}{9E} \bar{\sigma}^2 + \frac{T_{xy}^2}{1+\nu} , \quad A_2 = \sigma_x'^2 + 2\nu\sigma_x'\sigma_y' + \sigma_y'^2 , \\
A_3 &= 2(1-\nu^2)A_1 + A_2 , \quad \sigma_x = (2\sigma_x' - \sigma_y')/3 , \\
\sigma_y' &= (2\sigma_y' - \sigma_x')/3 , \quad H' = \bar{\Delta\sigma}/\bar{\Delta\epsilon}^P , \\
\bar{\sigma} &= [\sigma_x'^2 + \sigma_y'^2 - \sigma_x'\sigma_y' + 3T_{xy}'^2]^{1/2} \\
\bar{\Delta\epsilon}^P &= 2/3 [(\Delta\epsilon_x^P)^2 + (\Delta\epsilon_y^P)^2 + (\Delta\epsilon_z^P)^2 + \frac{1}{2} (\Delta\gamma_{xy}^P)^2]^{1/2} \quad (2)
\end{aligned}$$

and σ_0 is the yield stress in simple tension or compression. For an elastic element in which $\sigma < \sigma_0$, the constitutive matrix is

$$[D] = \frac{E}{1-\nu^2} \begin{bmatrix} 1 & \nu & 0 \\ \nu & 1 & 0 \\ 0 & 0 & (1-\nu)/2 \end{bmatrix} . \quad (3)$$

The stiffness matrix $[k]$ for a triangular element is represented by

$$[k] = [B]^T [D] [B] t \Delta \quad (4)$$

where t denotes the thickness and Δ is the area of the triangular. Four triangular elements are used to construct a quadrilateral element as shown in reference 5. The element stiffness matrix is determined by static condensation and the kinematical matrix is formed by averaging at the centroid of each element.

⁵Chen, P. C. T., "Numerical Solution of Gun Tube Problems in the Elastic-Plastic Range," Proceedings 1977 Army Numerical Analysis and Computer Conference, pp. 423-439.

The computer program developed for the plane stress elastic-plastic problems was a modification of the previous program for the axisymmetric case.^{4,5} The overlay feature was utilized for reducing the core storage requirement. A disk was used as an auxiliary storage device for the current element information and for solving the large system of equation by partition. A tape may be used to store the final results for output plotting and also for restarting this program from a point of completion of a given loading sequence. The computer used was an IBM 360 Model 44.

MODEL AND LOADING

A two-dimensional photoplastic model of aluminum block and polycarbonate ring was designed.¹ The breech ring was made of 0.12 inch thick LEXAN plate and the top of the ring was fixed. This material has a Poisson's ratio of 0.38 in the elastic state and a limiting value of 0.5 in the plastic state. The stress-strain (σ - ϵ) curve for LEXAN beyond the proportional limit can be described by the modified Ramberg-Osgood equation in the following form

$$E\epsilon/\sigma_B = \sigma/\sigma_B + (3/7)(\sigma/\sigma_B)^n \quad \text{for } \sigma_A < \sigma < \sigma_C \quad (5)$$

and the values of five parameters are $E = 325$ Ksi, $n = 11.5$, $\sigma_A = 6.2$ Ksi, $\sigma_B = 8.7$ Ksi, $\sigma_C = 9.576$ Ksi, where E is Young's modulus, n is a parameter,

¹Cheng, Y. F., "Photoplastic Study of Residual Stress in an Overloaded Breech Ring," Technical Report ARLCB-TR-78018, November 1978.

⁴Chen, P. C. T., "Elastic-Plastic Solution of a Two-Dimensional Tube Problem by the Finite Element Method," Transactions of Nineteenth Conference of Army Mathematicians, ARO Report 73-3, pp. 763-784, 1973.

⁵Chen, P. C. T., "Numerical Solution of Gun Tube Problems in the Elastic-Plastic Range," Proceedings 1977 Army Numerical Analysis and Computer Conference, pp. 423-439.

σ_A is the proportional limit, σ_B is the secant yield strength having a slope equal to $0.7 E$ and σ_C is the flow stress at which the slope of the stress-strain curve is zero. A piecewise linear representation for the effective stress-strain curve is used in this numerical study and the values for 11 data points other than the origin are

$$\begin{aligned}
 (\epsilon_1, \sigma_1 \text{ in Ksi}) = & (.018621, 6.), (.020401, 6.5), \\
 & (.022480, 7.0), (.025158, 7.5), (.028988, 8.0), \\
 & (.034934, 8.5), (.044635, 9.0), (.051679, 9.25), \\
 & (.060781, 9.50), (.064043, 9.596), (.1, 9.576) \quad . \quad (6)
 \end{aligned}$$

The dimensionless slope ω_1 is defined as

$$\omega_1 = E^{-1}(\sigma_{i+1} - \sigma_i) / (\epsilon_{i+1} - \epsilon_i) \quad (7)$$

and we can calculate $(H'/E)_1 = \omega_1 / (1 - \omega_1)$ for $i = 1, \dots, 10$.

A finite element representation for one half of the breech ring is shown in Figure 1. The other half is not needed because of symmetry. There are 224 grid points and 189 quadrilateral elements in this model. The grids 1 thru 8 are constrained in x-direction only while grids 217 thru 224 are held fixed. The top portion of the breech ring is omitted because it is believed to have little effect on the maximum stress information near the lower fillet. This belief has been confirmed by obtaining the elastic solution for another finite element model with an additional 70 quadrilateral elements in the top portion. The difference between these two models for the maximum tensile stress is only 1.3 percent. The aluminum block is regarded as rigid and the load is transmitted to the ring through contact. Initially, the block is in full contact with the ring. As the load increases, a gap develops in the central

portion. The width of the central gap under the full test load ($2F = 1144$ pounds) is observed experimentally to be about five inches. Our elastic-plastic finite element program in its present form cannot be used to determine the width of contact and the force distribution as functions of loading.

Guided by the experimental information on the width of central gap, we have chosen four contact conditions in this numerical investigation. The points of contact are at nodes (33, 41, 49, 57) for case 1, at nodes (41, 49, 57) for case 2, at nodes (49, 57, 65) for case 3 and at nodes (57, 65) for case 4. The width of contact and the force distribution in each case are assumed to remain unchanged during loading and only the total force ($2F$) is allowed to increase. The force distribution may be uniform or non-uniform and both types have been used in this study. Initially we apply a small force to obtain elastic solution and the total force ($2F^*$) required to cause incipient plastic deformation is calculated by using the von Mises' yield criterion. Then we apply the additional force in increments until the maximum test load is reached.

The load increments we chose are non-uniform because our experience indicates that smaller increments should be used as plastic deformation becomes larger. Our choice for the present investigation is an arithmetic decreasing sequence generated automatically in the program. If ten incremental steps are used, then

$$\Delta F_j = \frac{1}{145} \quad 19, 18, \dots, 11, 10 \quad (5.72 - F^*) \quad \text{for } j = 1, \dots, 10 \quad (8)$$

It is important to choose a proper set of increments in order to obtain good results at a reasonable cost. To reach the maximum test load of $2F = 1144$

pounds, we used 11 increments for the four contact conditions and 22 increments for the second and third cases. The difference between 11 and 22 incremental loadings for the maximum tensile stress is found to be within one percent. The restart feature of the program has been used for the second contact condition to increase the total force from 1144 pounds to 1300 pounds in seven additional steps. The increments are again non-uniform.

RESULTS AND DISCUSSIONS

The numerical results of the stresses in all elements were obtained for the overloaded breech ring under different contact conditions. Some of them are presented below in Figures 2 thru 7. The major principal stresses in elements along the contact region and fillet are shown in Figures 2 thru 5 for the four contact conditions under uniform load distributions. In each of these figures, we presented two sets of data corresponding to the load levels at the initial yielding (F^*) and at the maximum test load ($F = 572$ pounds). The incipient plastic deformation first occurs in element 99 for the first two cases and in element 50 for the last two cases. The values of load level for the four cases are $F^* = 312.8, 321.9, 221.7, 169.2$ pounds. The initial yielding is tensile in element 99 and compressive in element 50. It is interesting to find out that the location of the maximum tensile stress is in element 99 for all contact conditions under either uniform or non-uniform load distributions and this location remains unchanged as the total force increases. Since this location is of sufficient distance from the contact regions, it seems to suggest that Saint Venant's principle can be applied to this problem in the elastic as well as plastic range of loading.

The values of the maximum tensile stress based on the four contact conditions with uniform load distribution are 2029, 1972, 1939, 1936, psi at $F = 100$ pounds and 9532, 9361, 9174, 9119 psi at $F = 572$ pounds. It should be noted that the stresses in the finite element program were calculated at the centroid of each element but only one principal stress at the boundary was measured. The values of the maximum tensile stress at the fillet based on experimental approach are 2222 psi at $F = 100$ pounds and 9300 psi at $F = 572$ pounds.

For the purpose of comparison, the boundary stress is determined by extrapolation using the calculated results for those elements along the radial direction through element 99. This is illustrated in Figure 6 for the second case of contact condition. Similar figures for the other three cases are not shown. Three curves are plotted in Figure 6 and they represent the major principal stresses for three load levels at the initial yielding, maximum test load and complete unloading after reaching the maximum load. The residual stresses after complete unloading are determined by assuming that the unloading process is purely elastic. Our numerical results reveal no reverse yielding. In extrapolating the boundary stress, we shall remember that the maximum tensile stress shall not exceed the flow stress of 9576 psi. As seen in Figure 6, a comparison between the numerical and the experimental results for the maximum tensile stress indicates that a satisfactory agreement has been reached.

In Figure 7, two principal stresses as well as the residual stresses in element 99 are shown as functions of loading. Only the second case of contact conditions is presented here for illustration. The residual stress is

determined by assuming a purely elastic unloading resulting from various stages of loading. The minor principal stress (σ_2) is found to be a nearly linear function of loading and its residual value is very small. The value of the principal stress angle for all contact conditions and for all load levels is found to lie within -26° to -27° with respect to the x-axis. As can be seen in Figure 7, the major principal stress (σ_1) and its residual value increase in magnitude as the total contact force increases, but they are of opposite signs. Therefore, the production of compressive residual stress in an overloaded breech ring is beneficial because it can counteract the high operating tensile stress induced by firing. As a result of prestressing during the process of manufacturing, the elastic carrying capacity and fatigue life can be increased, and thus the chances of breech failures can be reduced. Furthermore, the finite element program developed here is a useful tool in redesigning breech rings or blocks.

REFERENCES

1. Cheng, Y. F., "Photoplastic Study of Residual Stress in an Overloaded Breech Ring," Technical Report ARLCB-TR-78018, November 1978.
2. Chen, P. C. T. and O'Hara, G. P., "NASTRAN Analysis of a Photoplastic Model for Sliding Breech Mechanism," Proceedings 1979 Army Numerical Analysis and Computer Conference, pp. 237-254.
3. Yamada, Y., Yoshimura, N., and Sakurai, T., "Plastic Stress-Strain Matrix and Its Application for the Solution of Elastic-Plastic Problems by the Finite Element Method," International Journal of Mechanical Science, Vol. 10, pp. 343-354, 1968.
4. Chen, P. C. T., "Elastic-Plastic Solution of a Two-Dimensional Tube Problem by the Finite Element Method," Transactions of Nineteenth Conference of Army Mathematicians, ARO Report 73-3, pp. 763-784, 1973.
5. Chen, P. C. T., "Numerical Solution of Gun Tube Problems in the Elastic-Plastic Range," Proceedings 1977 Army Numerical Analysis and Computer Conference, pp. 423-439.

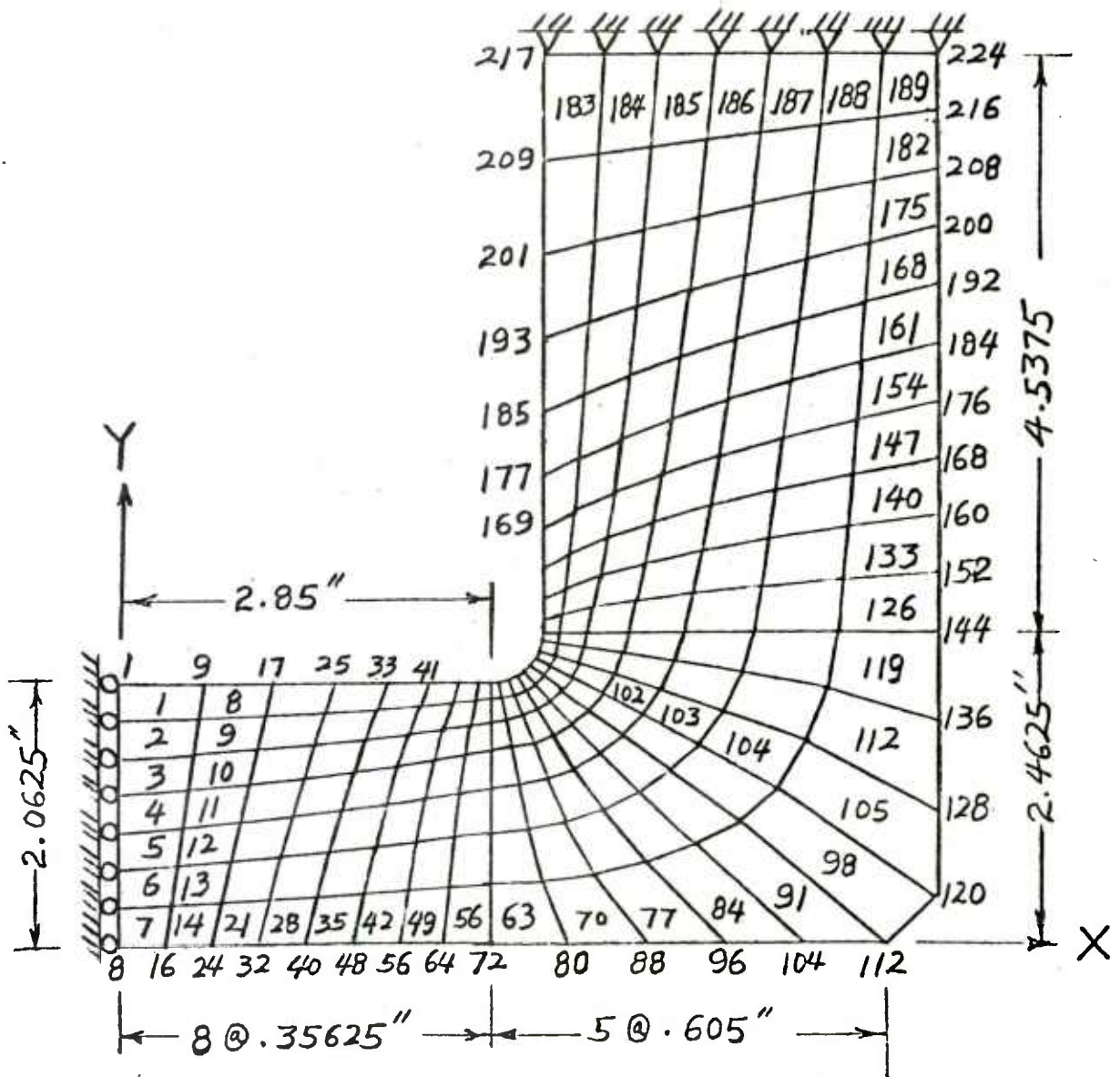


Figure 1. A Finite Element Model for Breech Ring

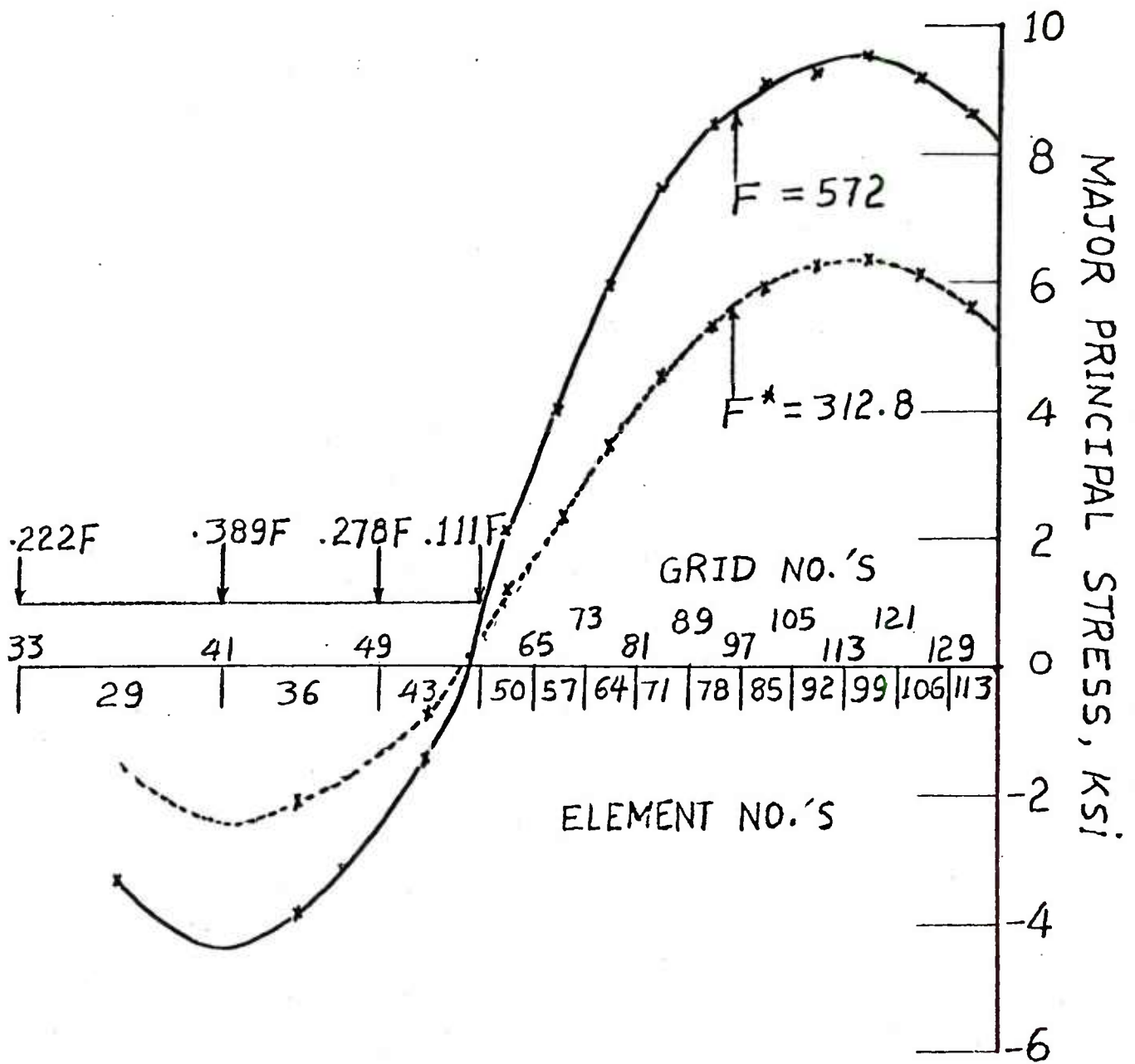


Figure 2. Major Principal Stress Along the Boundary Elements for Case 1

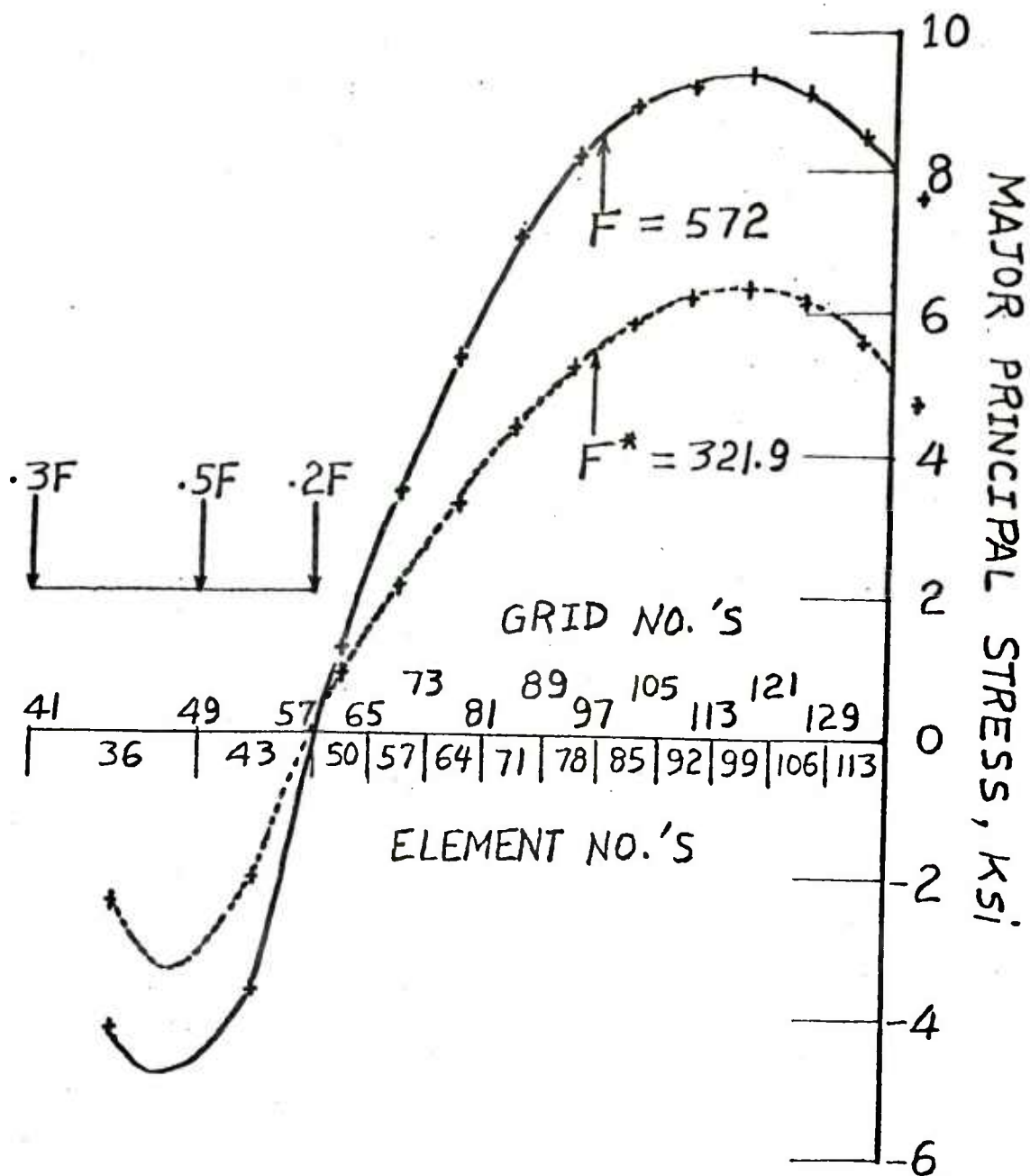


Figure 3. Major Principal Stress Along the Boundary Elements for Case 2

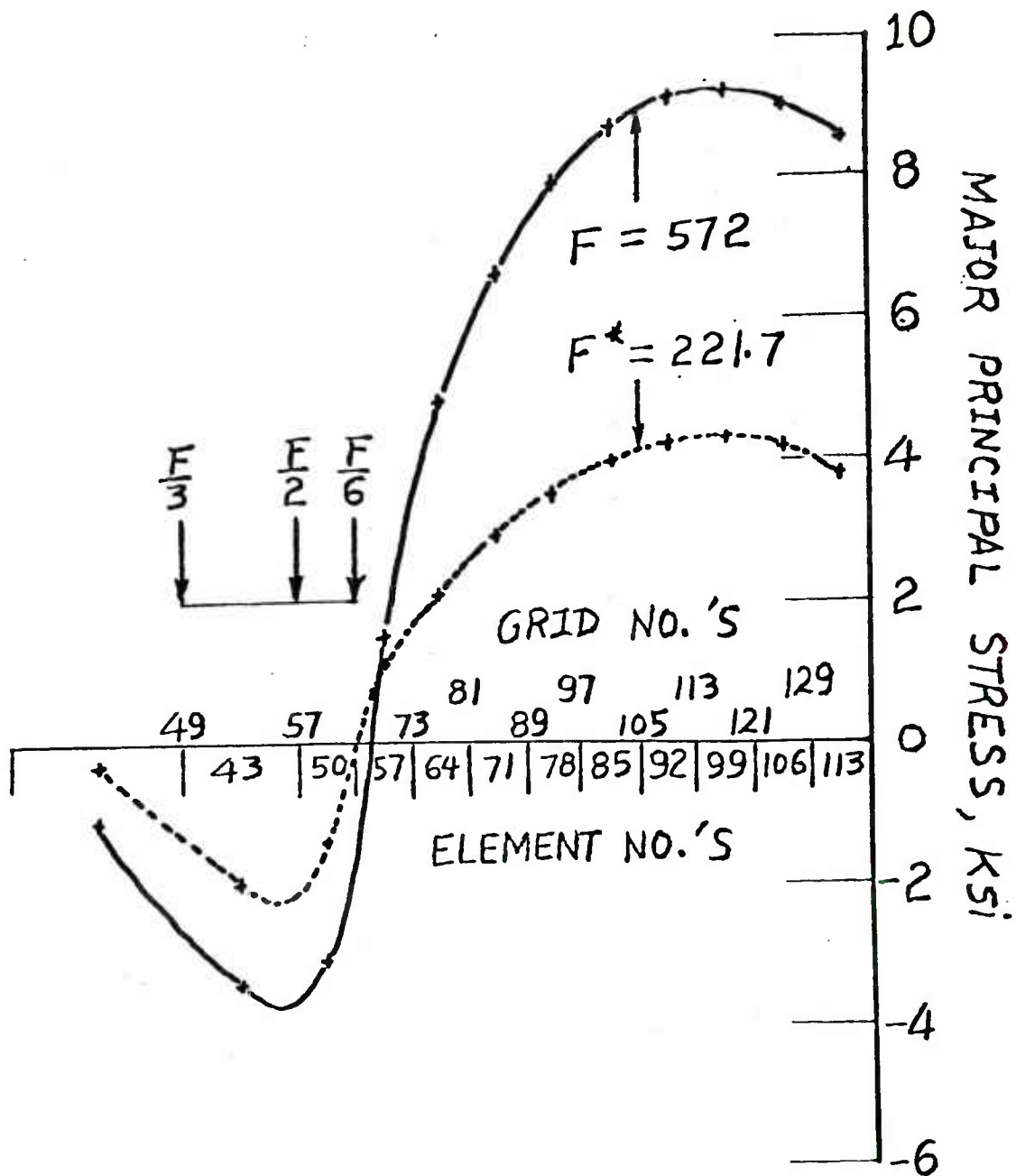


Figure 4. Major Principal Stress Along the Boundary Elements for Case 3

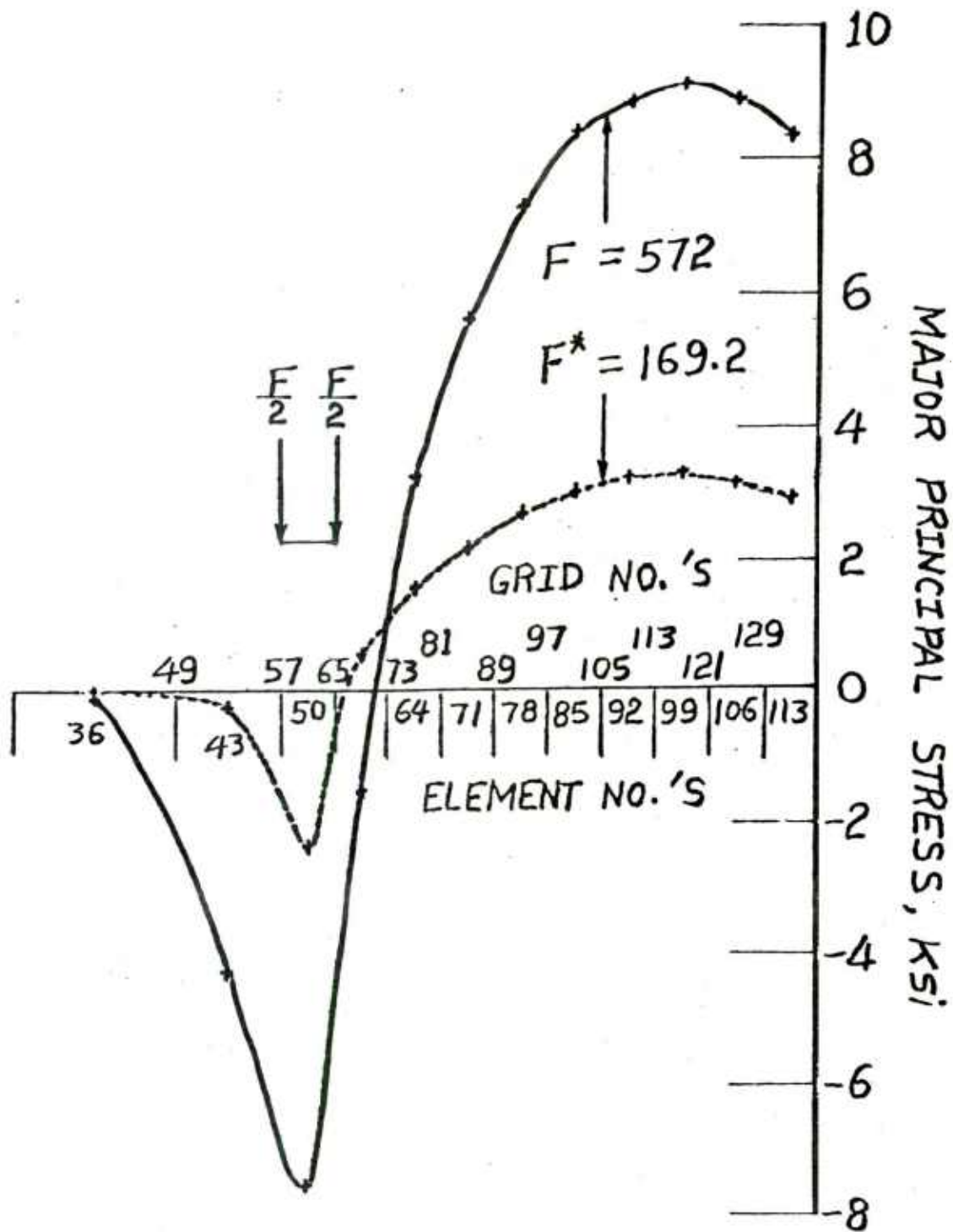


Figure 5. Major Principal Stress Along the Boundary Elements for Case 4

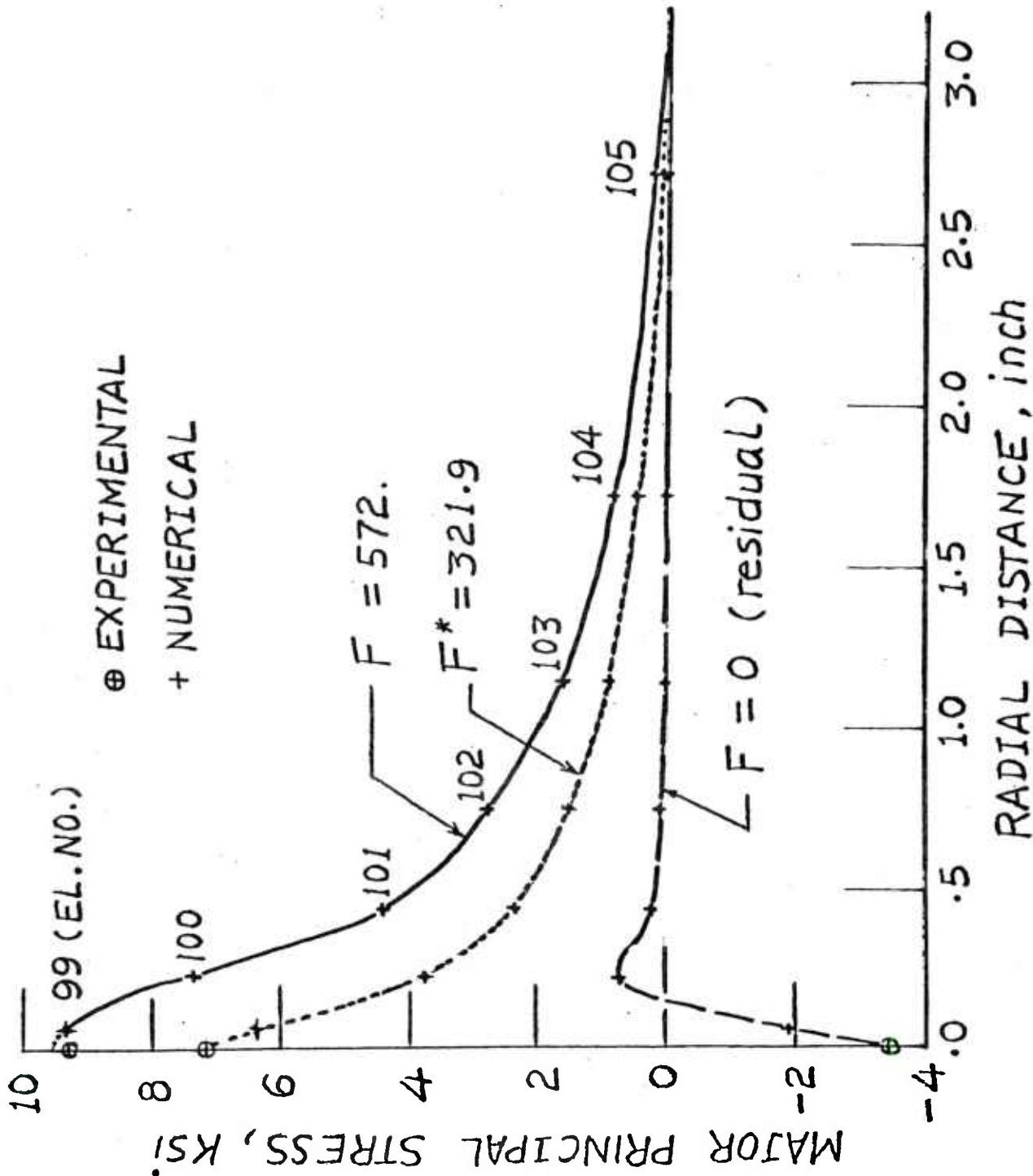


Figure 6. Determination of the Maximum Tensile Stress for Case 2

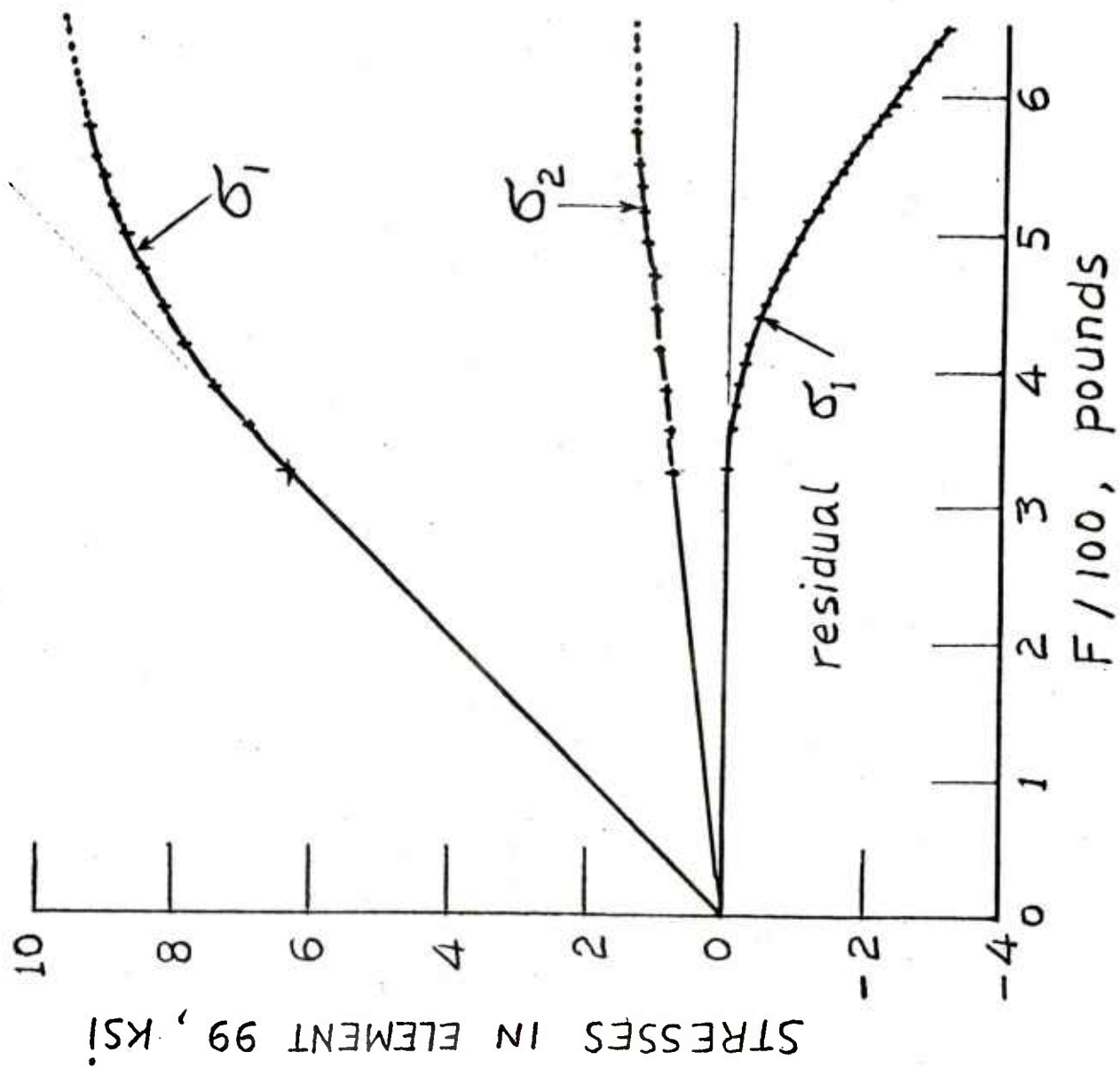


Figure 7. Stresses in Element 99 as functions of Contact Force for Case 2

TECHNICAL REPORT INTERNAL DISTRIBUTION LIST

	<u>NO. OF COPIES</u>
COMMANDER	1
CHIEF, DEVELOPMENT ENGINEERING BRANCH	1
ATTN: DRDAR-LCB-DA	1
-DM	1
-DP	1
-DR	1
-DS	1
-DC	1
CHIEF, ENGINEERING SUPPORT BRANCH	1
ATTN: DRDAR-LCB-SE	1
-SA	1
CHIEF, RESEARCH BRANCH	2
ATTN: DRDAR-LCB-RA	1
-RC	1
-RM	1
-RP	1
CHIEF, LWC MORTAR SYS. OFC.	1
ATTN: DRDAR-LCB-M	
CHIEF, IMP. 81MM MORTAR OFC.	1
ATTN: DRDAR-LCB-I	
TECHNICAL LIBRARY	5
ATTN: DRDAR-LCB-TL	
TECHNICAL PUBLICATIONS & EDITING UNIT	2
ATTN: DRDAR-LCB-TL	
DIRECTOR, OPERATIONS DIRECTORATE	1
DIRECTOR, PROCUREMENT DIRECTORATE	1
DIRECTOR, PRODUCT ASSURANCE DIRECTORATE	1

NOTE: PLEASE NOTIFY ASSOC. DIRECTOR, BENET WEAPONS LABORATORY, ATTN:
DRDAR-LCB-TL, OF ANY REQUIRED CHANGES.

TECHNICAL REPORT EXTERNAL DISTRIBUTION LIST

	<u>NO. OF COPIES</u>		<u>NO. OF COPIES</u>
ASST SEC OF THE ARMY RESEARCH & DEVELOPMENT ATTN: DEP FOR SCI & TECH THE PENTAGON WASHINGTON, D.C. 20315	1	COMMANDER US ARMY TANK-AUTMV R&D CMD ATTN: TECH LIB - DRDTA-UL MAT LAB - DRDTA-RK WARREN MICHIGAN 48090	1 1
COMMANDER US ARMY MAT DEV & READ. CMD ATTN: DRUDE 5001 EISENHOWER AVE ALEXANDRIA, VA 22333	1	COMMANDER US MILITARY ACADEMY ATTN: CHMN, MECH ENGR DEPT WEST POINT, NY 10996	1
COMMANDER US ARMY ARRADCOM ATTN: DRDAR-LC -ICA (PLASTICS TECH EVAL CEN)	1 1	COMMANDER REDSTONE ARSENAL ATTN: DRSMI-RB -RRS -RSM ALABAMA 35809	2 1 1
-ICE -LCM -LCS -LCW -TSS(STINFO)	1 1 1 1 2	COMMANDER ROCK ISLAND ARSENAL ATTN: SARRI-ENM (MAT SCI DIV) ROCK ISLAND, IL 61202	1
DOVER, NJ 07801			
COMMANDER US ARMY ARRCOM ATTN: DR SAR-LEP-L ROCK ISLAND ARSENAL ROCK ISLAND, IL 61299	1	COMMANDER HQ, US ARMY AVN SCH ATTN: OFC OF THE LIBRARIAN FT RUCKER, ALABAMA 36362	1
DIRECTOR US Army Ballistic Research Laboratory ATTN: DRDAR-TSB-S (STINFO) ABERDEEN PROVING GROUND, MD 21005.	1	COMMANDER US ARMY FGN SCIENCE & TECH CEN ATTN: DRXST-SD 220 7TH STREET, N.E. CHARLOTTESVILLE, VA 22901	1
COMMANDER US ARMY ELECTRONICS CMD ATTN: TECH LIB FT MONMOUTH, NJ 07703	1	COMMANDER US ARMY MATERIALS & MECHANICS RESEARCH CENTER ATTN: TECH LIB - DRXMR-PL WATERTOWN, MASS 02172	2
COMMANDER US ARMY MOBILITY EQUIP R&D CMD ATTN: TECH LIB FT BELVOIR, VA 22060	1		

NOTE: PLEASE NOTIFY COMMANDER, ARRADCOM, ATTN: BENET WEAPONS LABORATORY, DRDAR-LCB-TL, WATERVLIET ARSENAL, WATERVLIET, N.Y. 12189, OF ANY REQUIRED CHANGES.

TECHNICAL REPORT EXTERNAL DISTRIBUTION LIST (CONT)

	<u>NO. OF COPIES</u>		<u>NO. OF COPIES</u>
COMMANDER US ARMY RESEARCH OFFICE. P.O. BOX 12211 RESEARCH TRIANGLE PARK, NC 27709	1	COMMANDER DEFENSE TECHNICAL INFO CENTER ATTN: DTIA-TCA CAMERON STATION ALEXANDRIA, VA 22314	12
COMMANDER US ARMY HARVEY DIAMOND LAB ATTN: TECH LIB 2800 POWDER MILL ROAD ADELPHIA, ME 20783	1	METALS & CERAMICS INFO CEN BATTELLE COLUMBUS LAB 505 KING AVE COLUMBUS, OHIO 43201	1
DIRECTOR US ARMY INDUSTRIAL BASE ENG ACT ATTN: DRXPE-MT ROCK ISLAND, IL 61201	1	MECHANICAL PROPERTIES DATA CTR BATTELLE COLUMBUS LAB 505 KING AVE COLUMBUS, OHIO 43201	1
CHIEF, MATERIALS BRANCH US ARMY R&S GROUP, EUR BOX 65, FPO N.Y. 09510	1	MATERIEL SYSTEMS ANALYSIS ACTV ATTN: DRXSY-MP ABERDEEN PROVING GROUND MARYLAND 21005	1
COMMANDER NAVAL SURFACE WEAPONS CEN ATTN: CHIEF, MAT SCIENCE DIV DAHLGREN, VA 22448	1		
DIRECTOR US NAVAL RESEARCH LAB ATTN: DIR, MECH DIV CODE 26-27 (DOC LIB) WASHINGTON, D. C. 20375	1 1		
NASA SCIENTIFIC & TECH INFO FAC. P. O. BOX 8757, ATTN: ACQ BR BALTIMORE/WASHINGTON INTL AIRPORT MARYLAND 21240	1		

NOTE: PLEASE NOTIFY COMMANDER, APRADCOM, ATTN: BENET WEAPONS LABORATORY,
DRDAF-ICB-TL, WATERVLIET ARSENAL, WATERVLIET, N.Y. 12189, OF ANY
REQUIRED CHANGES.